Development of a Pharmacophore for Inhibition of Human Liver Cytochrome P-450 2D6: Molecular Modeling and Inhibition Studies

Günter R. Strobl,*,† Stephanie von Kruedener,‡ Joachim Stöckigt,‡ F. Peter Guengerich,§ and Thomas Wolff†

Institut für Toxikologie, GSF - Forschungszentrum für Umwelt und Gesundheit, 8042 Neuherberg, Germany, Institut für Pharmazie, Johannes Gutenberg-Universität, 6500 Mainz, Germany, and Center in Molecular Toxicology, Vanderbilt University, Nashville, Tennessee 37232

Received December 31, 1991

To gain insight into the specificity of cytochrome P-450 2D6 toward inhibitors, a preliminary pharmacophore model was built up using strong competitive inhibitors. Ajmalicine (1), the strongest inhibitor known (K_i = 3 nM) was selected as template because of its rigid structure. The preliminary pharmacophore model was validated by performing inhibition studies with derivatives of ajmalicine (1) and quinidine (9). Bufuralol (18) was chosen as substrate and the metabolite 1'-hydroxybufuralol (19) was separated by high performance liquid chromatography. All incubations were carried out using human liver microsomes after demonstration that the K_i values obtained with microsomes were in accordance with those obtained with a reconstituted monooxygenase system containing purified cytochrome P-450 2D6. Large differences of K_i values ranging between 0.005 and 100 μM were observed. Low-energy conformers of tested compounds were fit within the preliminary pharmacophore model. The analysis of steric and electronic properties of these compounds led to the definition of a final pharmacophore model. Characteristic properties are a positive charge on a nitrogen atom and a flat hydrophobic region, the plane of which is almost perpendicular to the N-H axis and maximally extends up to a distance of 7.5 Å from the nitrogen atom. Compounds with high inhibitory potency had additional functional groups with negative molecular electrostatic potential and hydrogen bond acceptor properties on the opposite side at respective distances of 4.8-5.5 Å and 6.6-7.5 Å from the nitrogen atom. The superposition of strong and weak inhibitors led to the definition of an excluded volume map. Compounds that required additional space were not inhibitors. This is apparently the first pharmacophore model for inhibitors of a cytochrome P-450 enzyme and offers the opportunity to classify compounds according to their potency of inhibition. Adverse drug interactions which occur when both substrates and inhibitors of cytochrome P-450 2D6 are applied may be predicted.

Introduction

Human liver cytochrome P-450 enzymes are known to oxidize a variety of exogenous and endogenous compounds.[1] The oxidation products themselves are substrates of conjugating enzymes like glucuronosyltransferases, sulfotransferases, or hydrolases, and are converted to hydrophilic, easily excretable metabolites. Generally, cytochrome P-450 enzymes catalyze the rate-limiting step of the total metabolism. As for drugs, this means that their activities determine plasma concentrations and consequently, therapeutic and toxic responses.

Cytochrome P-450 2D6 oxidizes more than 20 drugs, among them antihypertensives (e.g. debrisoquine), β-adrenergic blockers, (e.g. bufuralol, metoprolol, alprenolol), antiarrhythmics, (e.g. sparteine, encainide, *N*-propylajmaline), and antidepressants (e.g. amitriptyline, desipramine, amiflamine).[2,3] The activity of this enzyme may be low in some individuals because of either genetic polymorphism or interaction with strong inhibitors. Five to ten percent of the European and North American Caucasian population are deficient in this enzyme.[4-6] If those poor metabolizers are repeatedly treated with a drug that is a substrate of the enzyme, an accumulation of the compound will occur. As a consequence, exaggerated responses and serious and even life-threatening toxic effects can be expected and have been reported by several authors.[7-9] Similar responses may occur in extensive metabolizers if a strong inhibitor of cytochrome P-450 2D6 competes with a substrate for the active site of the enzyme. For example, quinidine (9) is a strong competitive inhibitor in vitro (K_i = 60 nM)[10] as well as in vivo. Quinidine administration may even lead to an alteration in the phenotype, i.e. extensive metabolizers of debrisoquine and other substrates become poor metabolizers of these drugs during quinidine treatment.[11-14]

Our aim was to define the specificity of cytochrome P-450 2D6 toward inhibitors by developing a pharmacophore model. At the beginning of our study inhibition constants had been determined in vitro for a number of compounds using human liver microsomes.[15-17] Microsomes also contain other enzymes besides cytochrome P-450 2D6, and therefore K_i values determined with this cell fraction have to be regarded as apparent inhibition constants. In case of a high affinity of the tested compound for a different enzyme, the concentration available for inhibition of cytochrome P-450 2D6 might be markedly lower than the applied concentration, and K_i values might be overestimated. In order to check if K_i values determined with microsomes are a reliable database for computer-aided molecular modeling, cytochrome P-450 2D6 had to be purified and inhibitory studies had to be performed with the reconstituted enzyme. If K_i values determined with microsomes are reliable, then common structural features of inhibitors may be defined. Molecular modeling offers

* Address of correspondence: E. Merck, Institut für Toxikologie, 6100 Darmstadt, Germany.
† Institut für Toxikologie, GSF - Forschungszentrum für Umwelt und Gesundheit.
‡ Institut für Pharmazie, Johannes Gutenberg-Universität.
§ Center in Molecular Toxicology, Vanderbilt University.

0022-2623/93/1836-1136$04.00/0

a variety of tools to build up structures and gain insight into the flexibility and the electrostatic potential of molecules.[18,19] Interactive superposition and superposition using least squares fit methods make possible the determination of enzyme-bound conformers and the development of a pharmacophore model. It is only likely to arrive at that end however, if the potencies of inhibition do not depend on physicochemical properties such as partition coefficients only, but also on structural properties, and if an inhibitor having a rather rigid structure can be used as a template, because only in this case functional groups have a defined arrangement. As for cytochrome P-450 2D6, both prerequisites are fulfilled. First, the enzyme seems to have a distinct specifity toward inhibitors: quinidine (9) and quinine (10) which are stereoisomers and hardly differ in their physicochemical properties, are known to differ in their inhibitory potency by 2 orders of magnitude.[10] Second, it is known that the indole alkaloid ajmalicine (1), which is a highly potent inhibitor of the enzyme,[17] has a rather rigid structure.

Biochemical Studies

Inhibition studies were carried out using human liver microsomes and reconstituted cytochrome P-450 2D6 which had been partially purified. The preparation of microsomes was described by Guengerich,[20] the purification of the enzyme was done according to Distlerath et al.[21] The potency of compounds to inhibit cytochrome P-450 2D6-dependent reactions was determined by measuring the amount of 1′-hydroxybufuralol (19) formed in the presence of bufuralol (18) and an NADPH-regenerating system and evaluation of the data according to Dixon.[22] The separation of the metabolite was achieved by high performance liquid chromatography.[23]

Molecular Modeling

Computer-assisted molecular modeling studies were carried out using the workstation IRIS 4D/50GT (Silicon Graphics, Munich, Germany) and a CONVEX C220 (Convex, Munich, Germany). The structures of inhibitors were read in from the Cambridge Crystallographic Data Base[24] or built up interactively using the SYBYL program.[25] After a full geometry optimization, partial atomic charges were calculated with MNDO.[26] Energy minimizations were done by means of the MAXIMIN2 option of SYBYL (method: conjugate-gradient; termination option: gradient; rms-gradient: 0.002 kcal/mol A^2). All force field calculations were carried out considering electrostatic interactions. For consistency, all energy values were calculated with version 5.3 of SYBYL. Conformational analysis was carried out using the SEARCH option of SYBYL. The procedure applied was dependent on the number of rotatable bonds within the molecule. The torsional angles of terminal alkyl groups were only studied when intramolecular steric interactions were to be expected. In case of one or two rotatable bonds conformational space was searched using 10° increments. In case of three or more rotatable bonds 30° increments were applied to limit the number of conformations. In the latter case further searches were started in the ±30° environment of low-energy conformers using 10° increments. To make sure that all relevant conformers were taken into account, an energy limit as high as 50 kcal/mol was chosen in SYBYL SEARCH. Low-energy conformers were then energy minimized (conditions see above) and for superpositions, only those conformers were chosen whose energy was not more than 5 kcal/mol higher than that of the lowest-energy conformer.

Molecular electrostatic potentials were calculated for optimized structures using the POTENTIALS option of SYBYL on the basis of the MNDO point charges. Molecular dynamics calculations were carried out by means of the DYNAMICS option of SYBYL. In general, 400 000 time steps (400 ps) were computed at a constant temperature of 300 K after the molecule had been brought to that temperature within 600 time steps. Periodic boundary conditions were not applied.

Table I. Effect of Various Compounds on 1′-Hydroxybufuralol (19) Formation by Human Liver Microsomes and by Partially Purified Cytochrome P-450 2D6

compound	apparent K_i (μM)[a]	
	microsomes	purif P-450 2D6
ajmalicine (1)	0.014	0.0057
yohimbine (4)	0.23	0.52
quinidine (9)	0.040	0.043
quinine (10)	5.5	15
cinchonine (9b)	1.0	2.6
cinchonidine (10b)	9.3	25

[a] K_i values were obtained by graphical evaluation of Dixon plots. The incubations were carried out using three different substrate concentrations and five different inhibitor concentrations. All points were determined in duplicate. When experiments were repeated, K_i values maximally differed by a factor of 2. K_i values determined with microsomes of different liver donors differed by a factor of 1.3 to 3 depending on the inhibitor tested. The turnover number of the four microsomal preparations used were 0.29, 0.93, 0.31, and 0.22 nmol 19/nmol P-450 per min, respectively, the corresponding K_m values were 21, 17, 23, and 39 μM, respectively.

Results and Discussion

Reliability of K_i Values Determined with Microsomes and (±)-Bufuralol (18) as Substrate. Cytochrome P-450 2D6 makes up only a small fraction of human liver cytochromes P-450.[27] Different cytochrome P-450 enzymes and other proteins may also bind compounds tested as inhibitors of cytochrome P-450 2D6. Thus, the apparent K_i values determined with microsomes may not represent K_i values valid for the enzyme itself. Therefore, for a series of compounds, inhibition constants were determined both with microsomes and with partially purified cytochrome P-450 2D6 reconstituted with NADPH-cytochrome P-450 reductase and L-α-dilauroyl-*sn*-glycero-3-phosphocholine, using 1′-hydroxylation of 18 as a test reaction. In general, K_i values obtained with microsomes were 2 to 3 times lower than K_i values obtained with the reconstituted monooxygenase system (Table I). These differences were, however, in the range of the biological variation determined with microsomes from four liver donors (Table I). The results indicate that it is justified to use values obtained with microsomes as a database for molecular modeling analysis.

To determine if the K_i values determined with (+)-bufuralol (18a) and (−)-bufuralol (18b) are corresponding, incubations were carried out with several inhibitors in the presence of each of the two enantiomers and the racemic mixture. K_i values obtained with 18b were up to 4 times higher than K_i values obtained with 18a (Table II). The ranking of the potency of the inhibitors was independent of the enantiomer used as substrate. The results indicate that it is justified to use K_i values determined with racemic bufuralol (18) as a database for molecular modeling analysis.

Table II. Inhibition of 1′-Hydroxylation of (+)-Bufuralol (**18a**),[b] (−)-Bufuralol (**18b**),[c] and (±)-Bufuralol (**18**) in Microsomes

compound	K_i[a] (μM) [18a]	K_i[a] (μM) [18b]	K_i[a] (μM) [18]	$\frac{K_i\text{[a] [18b]}}{K_i\text{[a] [18a]}}$
ajmalicine (**1**)	0.0035	0.013	0.0046	3.7
yohimbine (**4**)	0.14	0.19	0.18	1.4
cinchonine (**9b**)	3.5	5.4	3.5	1.5
cinchonidine (**10b**)	7.3	16	7.5	2.2
10,11-Dihydrocinchonine (**9e**)	2.8	3.2	1.6	1.1
10,11-Dihydrocinchonidine (**10g**)	9.6	24	8.0	2.5

[a] K_i: apparent inhibition constant. [b] Turnover number: 0.48 nmol **18a**/nmol P-450 per min; K_m: 48 μM. [c] Turnover number: 0.20 nmol **18b**/nmol P-450 per min; K_m: 14 μM.

Table III. Inhibition Constants of Strong Inhibitors of Cytochrome P-450 2D6

inhibitor	K_i (μM)
ajmalicin (**1**)	0.0033[a]
chinidin (**9**)	0.060[b]
chlorpromazin (**13**)	7.0[c]
trifluperidol (**14**)	0.17[a]
prodipin (**15**)	0.0048[a]
lobelin (**16**)	0.12[a]

[a] From ref 17. [b] From ref 10. [c] From ref 15.

Development of a Preliminary Pharmacophore Model. In order to define common structural features of inhibitors of cytochrome P-450 2D6, only the structures of competitive inhibitors were included in the analysis, because only in this case one can assume that the molecules are interacting with the active site of the enzyme. In the first step only strong inhibitors were included. One member out of each class of compounds showing inhibition constants below 7 μM was chosen. The selection was the indole alkaloid ajmalicine (**1**), the cinchona alkaloid quinidine (**9**), the phenothiazine chlorpromazine (**13**), trifluperidol (**14**), prodipine (**15**), and lobeline (**16**). The inhibition constants are listed in Table III.

Every strong inhibitor possesses at least one aromatic ring and a basic nitrogen atom that is protonated under physiological conditions. Conformational analyses were carried out to determine if a common arrangement of these groups exists among the low-energy conformers of the molecules. The aromatic rings of the inhibitors should be preferentially coplanar. Therefore two points were defined on the normal to the ring plane going through the center of the ring. The distance between these points and the center was set to 1.7 Å, which is approximately the value of the van der Waals radius of aromatic carbon atoms. Besides the nitrogen atom, the hydrogen atom bound to it at physiological pH was included in superpositions. Its orientation is of great importance for the affinity of the molecule to the active site because of the strong electrostatic interaction. Taken together, the orientation in space of four points had to be checked in every superposition.

Ajmalicine (**1**) was chosen as a template because its structure seemed to be rather rigid. Molecular dynamics calculations were performed with the unprotonated molecule and the results suggest that only two conformers (A and B) exist, that differ in the orientation of the nitrogen atom (Figure 1). To determine which of the two conformers is probable to be the enzyme-bound one, low-energy conformers of the other inhibitors (see supplementary material for results of conformational analyses) were superimposed on conformers A and B of protonated ajmalicine (**1**). The four points of **13**–**16** overlapped with the four points of conformer A only. Because of two reasons, the vinyl group of quinidine (**9**) was superimposed with the aromatic rings of the other inhibitors instead of superimposing an aromatic ring of the quinoline system. First, the π-electrons of the double bond give rise to a negative molecular electrostatic potential in a corresponding region and second, there are polar groups in two regions

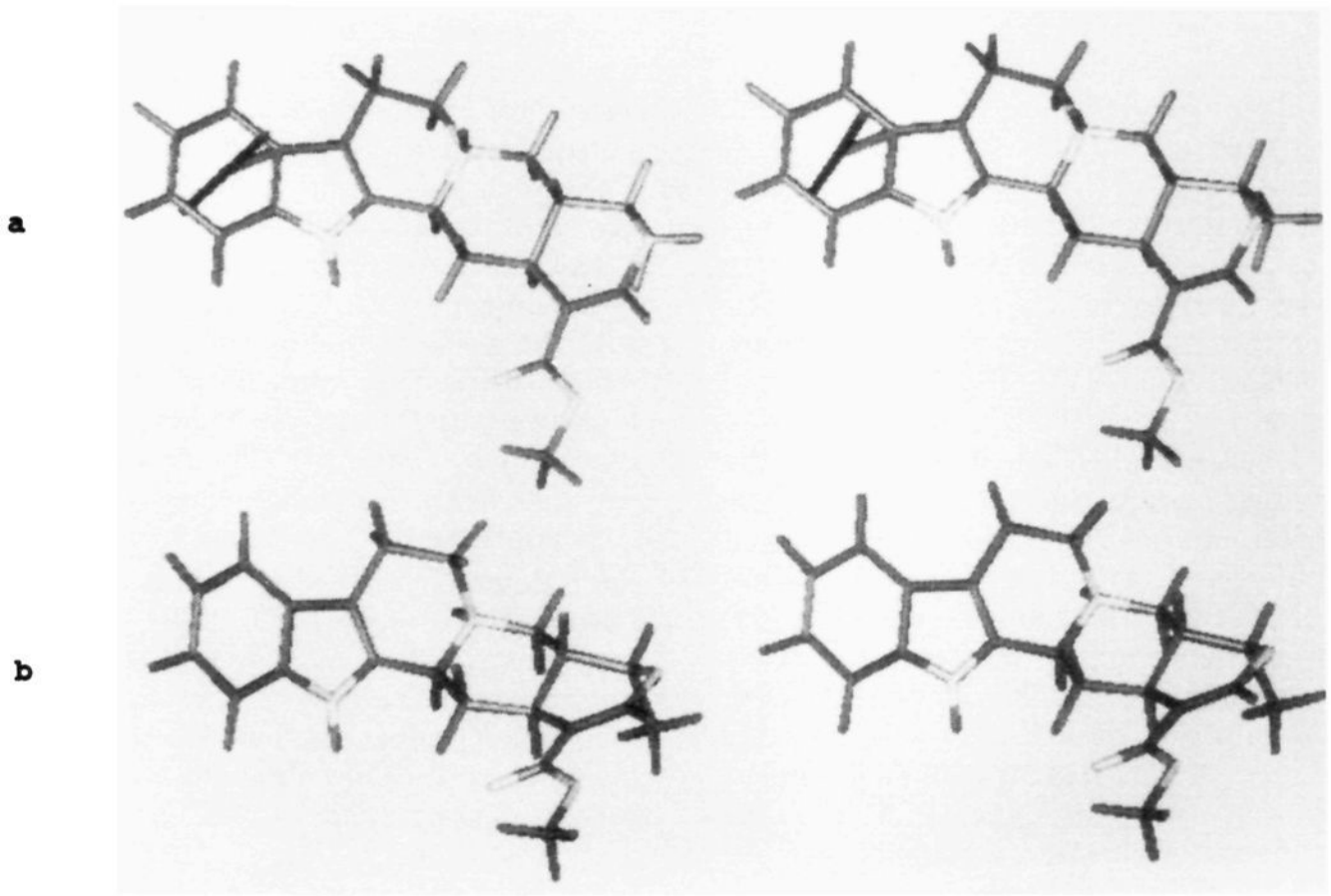

Figure 1. Stereoview of two conformers of protonated ajmalicine (**1**). (a) Conformer which corresponds to the X-ray structure of tetraphylline (11-methoxyajmalicine, **1e**). (b) Conformer formed by inversion of the (unprotonated) nitrogen tetrahedron.

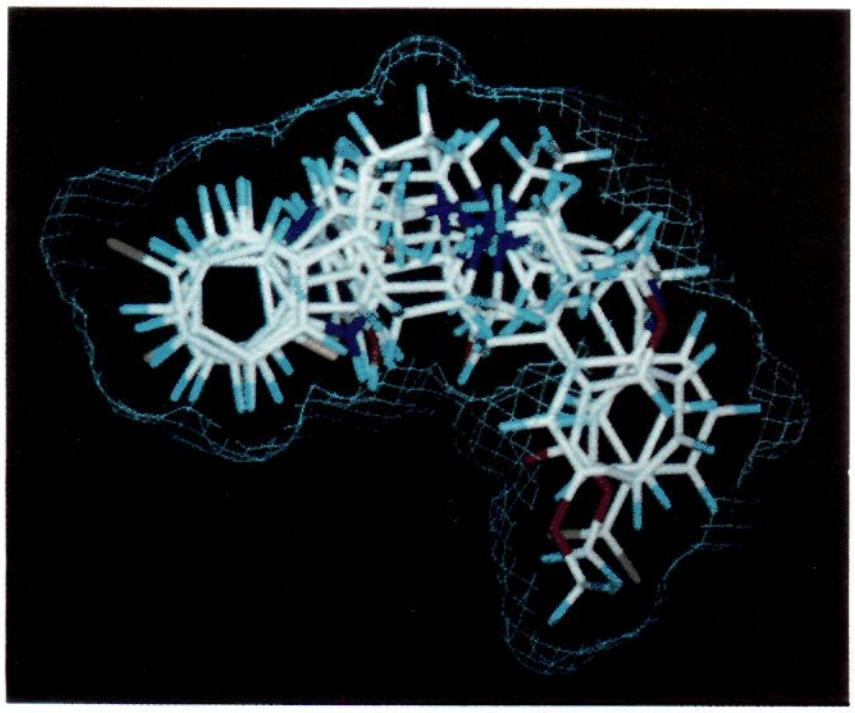

Figure 2. Superposition of ajmalicine (**1**), quinidine (**9**), chlorpromazine (**13**), trifluperidol (**14**), propidine (**15**), and lobeline (**16**). The Z-clipped grid represents the overall surface of the structures shown. Colors: C: white: H: cyan; N: dark blue; O: red; S: yellow; F, Cl: green.

of **9** that can be fit with analogous groups of **1** and **14**. The nitrogen atom of quinoline system of **9** lies close to the oxygen atom in ring E of **1**, and the methoxy group of **9** lies in the same region as the ester group of **1** and the trifluoromethyl group of **14** (Figure 2). All these polar groups show a negative molecular electrostatic potential.

Taken together, a preliminary pharmacophore model could be defined as follows: a tertiary nitrogen atom that is protonated to a high degree at physiological pH and a flat hydrophobic region (A) (Figure 3), the plane of which is almost perpendicular to the N–H axis and which has a negative molecular electrostatic potential perpendicular to that plane. Additional functional groups with lone pairs in region B seemed to cause an enhanced inhibitory potency. Hydrophobic groups in region C seemed to be allowed but not to cause an enhanced inhibitory potency.

Validation and Refinement of the Preliminary Pharmacophore Model. The definition of common structural features was a first hypothesis which had to be tested thoroughly. To this end, inhibitory studies were performed with derivatives of ajmalicine (**1**), which is the strongest inhibitor known, and of the cinchona alkaloid quinidine (**9**). Low-energy conformers of these derivatives were then fit within the pharmacophore model.

Indole Alkaloids. The relatively rigid structure of **1** and other indole alkaloids made this class of compounds especially suited for this study. In general a variation of substituents had only little influence on the overall structure of these compounds. The results of the inhibition studies are presented in Table IV. Compounds which are partial structures of **1** were only weak inhibitors (**6c**, **7a**, **7b**, **8**) or inhibited uncompetitively (**6a**, **6b**). None of them either has a tertiary basic nitrogen atom or groups with lone pairs in a region (B) where **1** has two. Since 5-methoxytryptamine (**6c**) has at least a basic aliphatic nitrogen atom, the low inhibitory potency further supports the assumption that additional hydrophobic interaction and hydrogen bond accepting groups in region B are necessary for a compound to be a strong inhibitor.

To examine the importance of the oxygen atom in ring E of **1** as a hydrogen bond accepting group, derivatives of **1** were tested that had the oxygen oriented differently or did not possess it at all. Tetrahydroalstonine (**1b**), which

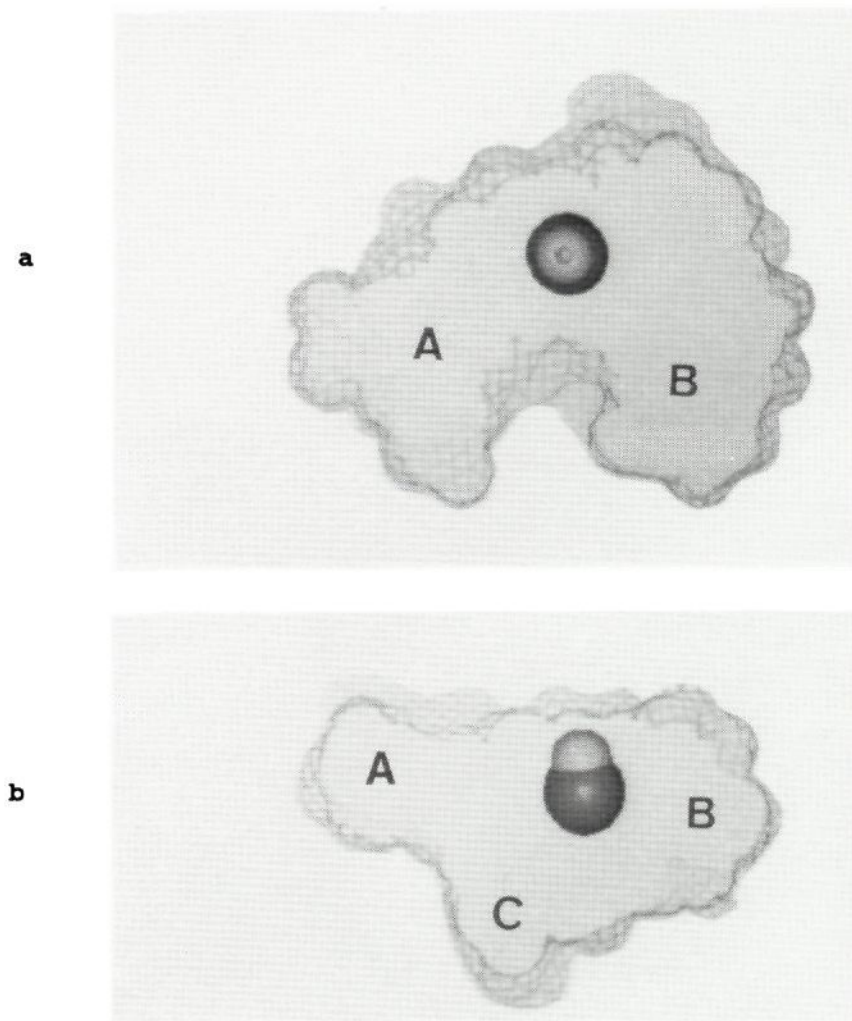

Figure 3. View of a Z-clipped grid which represents the overall surface of strong inhibitors. Note the position of the protonated nitrogen atom (spacefill; N: dark; H: bright). (a) Top view of the molecule plane; (b) after 90° turn around the x axis. Characteristic regions are denoted by capital letters.

differs from **1** only in the stereochemistry at carbon 20, and its nitrogen analogue **1c** were less potent than **1** by 3 orders of magnitude. Since the α-configuration at carbon 20 of **1b** and **1c** influences not only the orientation of the lone pairs at the heteroatom of ring E but also the orientation of the methyl group at C19, 19-epiajmalicine (**1d**) was tested because its methyl group is oriented similarly to that of **1b** and **1c**. The K_i value of **1d** was only slightly higher than that of **1** indicating that the reduced potency of **1b** and **1c** is mainly due to an unfavorable orientation of lone pairs. The K_i values obtained with yohimbine (**4**) and derivatives of it (**4a**, **4b**, **4c**, **5**), all of which are missing the oxygen atom in ring E, were 1 to 4 orders of magnitude less potent than **1**. These findings further support the importance of a hydrogen bond acceptor group for a high affinity to the active site. β-Yohimbine (**4c**) was the strongest inhibitor of this series, most probably because one lone pair of the 17α-hydroxyl group lies close to one lone pair of the ring oxygen atom of **1** (Figure 4).

The preliminary model had suggested that strong inhibitors have groups with a negative electrostatic potential that are able to form hydrogen bonds with active site amino acids also in a second area of region B. 16α-(Hydroxymethyl)-17α-hydroxyyohimban (**4a**) was more than 1 order of magnitude less potent than the 16-carbonic acid methyl ester **4**, and 16,17-didehydro-16-(hydroxymethyl)-19α-methyloxayohimban (**1a**) was more than 2 orders of magnitude less potent than **1**. These findings further supported the preliminary model and indicate that in this area substituents with pure hydrogen bond acceptor properties and low polarity are favored.

The comparison of the six strong inhibitors (**1**, **9**, **13**–**16**) had led to the conclusion that a basic nitrogen atom is essential for inhibition. This notion is supported by the

Table IV. Inhibitory Effects of Indole Alkaloids on Bufuralol 1′-Hydroxylation by Human Liver Microsomes

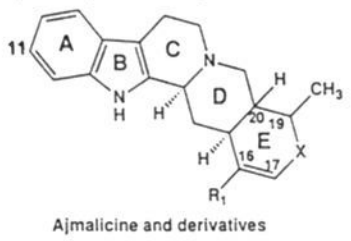

Ajmalicine and derivatives

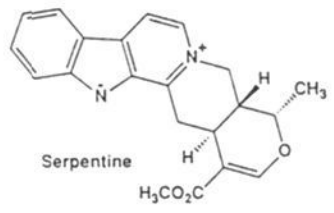

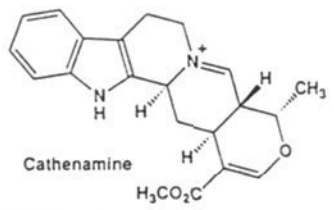

inhibitor	K_i^a (μM)	X	R_1	conformation at C19	conformation at C20
ajmalicine (**1**)	0.0046	O	CO_2CH_3	β	β
1a	1.1	O	CH_2OH	β	β
tetrahydroalstonine (**1b**)	5.0	O	CO_2CH_3	β	α
1c	2.9	N	CO_2CH_3	β	α
19-epiajmalicine (**1d**)	0.017	O	CO_2CH_3	α	β
serpentine (**2**)	2.2				
cathenamine (**3**)	3.2				

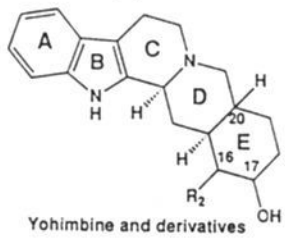

Yohimbine and derivatives

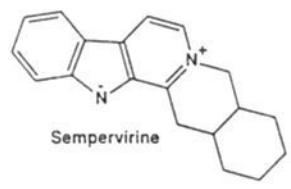

Sempervirine

inhibitor	K_i^a (μM)	R_2	conformation at C16	conformation at C17	conformation at C20
yohimbine (**4**)	0.18	CO_2CH_3	β	β	β
4a	6.3	CO_2OH	β	β	β
corynanthine (**4b**)	0.080	CO_2CH_3	α	β	β
β-yohimbine (**4c**)	0.031	CO_2CH_3	β	α	β
sempervirine (**5**)	9.7				

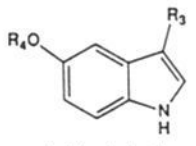

Indole derivatives

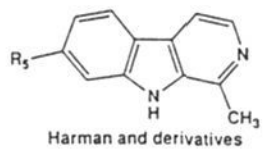

Harman and derivatives

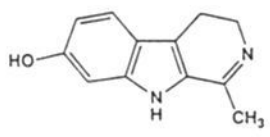

Harmalol

inhibitor	K_i^a (μM)	R_3	R_4	R_5
5-hydroxyindole (**6a**)	*b*	H	H	
5-methoxyindole (**6b**)	*b*	H	CH_3	
5-methoxytryptamine (**6c**)	100	CH_2CH_2OH	CH_3	
harman (**7a**)	86			H
harmine (**7b**)	50			OCH_3
harmalol (**8**)	65			

[a] K_i: apparent inhibition constant. [b] Uncompetitive inhibition.

fact that steroids and other compounds that do not take more space than inhibitors but that do not possess a basic nitrogen atom were not inhibitors.[17] The finding however, that serpentine (**2**), cathenamine (**3**), and sempervirine (**5**), all of which possess an iminium atom instead of a basic nitrogen atom, were competitive inhibitors, demanded a modification of the pharmacophore. It is probably the presence of a positive charge that is necessary for inhibition of cytochrome P-450 2D6. The higher potency of basic amines suggests that upon binding, the positive charge present in the protonated state is oriented towards the carboxylic group of an active site amino acid. In this case a higher interaction energy will result than with iminium derivatives, where the positive charge is not directed.

Cinchona Alkaloids. Chinchona alkaloids are a class of compounds the structures of which are more flexible

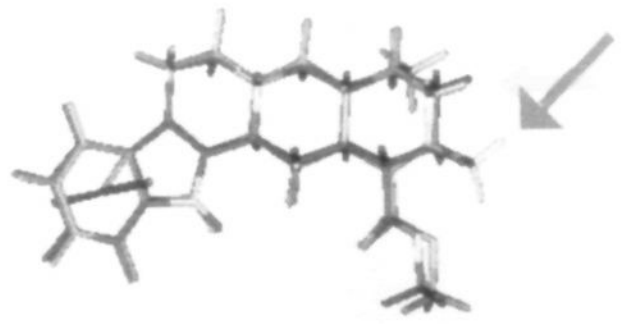

Figure 4. Superposition of β-yohimbine (**4c**) and ajmalicine (**1**). The bright arrow points toward a lone pair of **1**, the dark arrow toward a lone pair of **4c**.

than those of **1** and its derivatives. Quinoline and quinuclidine derivatives which are partial structures of cinchona alkaloids (**11**, **12a**, **12b**) did not inhibit bufuralol 1′-hydroxylation up to a concentration of 500 μM (Table V). These observations support the pharmacophore hypothesis because the structures of these compounds did not meet the prerequisites defined herein.

In order to determine low-energy conformations of quinidine (**9**) and quinine (**10**), conformational analyses of three rotatable bonds were carried out, two at the methylene bridge and one at the hydroxyl group to avoid bad van der Waals contacts. The results supplied no explanation for the difference in the K_i values of the enantiomers, because the conformers obtained were quite similar. In X-ray structures of **10** and its derivatives[28,29] however, the quinuclidine ring is located on the opposite side of the quinoline ring compared to **9** and its derivatives[30–33] (Figure 5). The low-energy conformer of **10** that corresponds to the X-ray structure can be fit within the pharmacophore model, but the orientation of hydrogen bond acceptor groups differs from that of **1** and **9** (Figure 6). In order to gain insight into the significance of the rotational barrier, molecular dynamics calculations were carried out for **9** and **10** taking the X-ray conformers as starting structures. In both cases, no rotation to the opposite side was observed (Figure 7). Similar results were obtained for the unprotonated compounds. NMR studies[34,35] had shown that the quinuclidine rings of the enantiomers were oriented in opposite directions also in solution. Taking together, these findings suggest that the lower inhibitory potency of **10** is due to the lack of groups that enhance activity in region B. Additional support for this explanation was obtained from studies with the desmethoxy and chloro derivatives of **9** and **10**. Only in the case of the desmethoxy derivative of quinidine (cinchonine, **9b**), which lacks a group enhancing activity, a sharp decline of the inhibitory potency was observed; for quinine (**10**) and its derivatives (**10b**, **10c**) similar K_i values were obtained. The fact that the quinidine analogue 6′-chlorocinchonine (**9c**) was a weaker inhibitor than **9** by almost 1 order of magnitude suggests that there is a cleft at the active site of cytochrome P-450 2D6 that can accommodate and interact best with a short alkoxy group. Further evidence for the existence of this cleft is provided by the earlier finding that **1**, exhibiting an ester group in a corresponding area, was much more effective than **1a**, which has the hydroxyl group instead of the ester group.

To test the influence of the configuration at carbon C9, K_i values and low-energy conformations of 9-epiquinidine (**9a**) and 9-epiquinine (**10a**) were determined. The structure of **10a** is rather rigid because strong electrostatic interactions exist between the amino and the hydroxyl group, both in the protonated and in the unprotonated state. This lowest-energy conformer resembles the con-

Table V. Inhibitory Effects of Cinchona Alkaloids on Bufuralol (18) 1′-Hydroxylation by Human Liver Microsomes

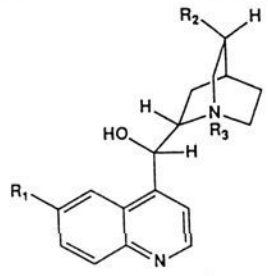

Quinidine/quinine and derivatives

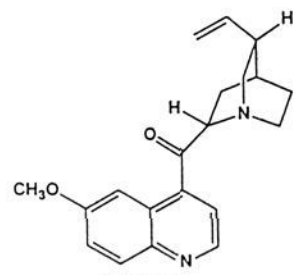

Quininone

inhibitor	K_i[a] (μM)	configuration at C8	configuration at C9	R_1	R_2	R_3
quinidine (**9**)	0.08	*R*	*S*	OCH_3	C_2H_3	–
quinine (**10**)	4.6	*S*	*R*	OCH_3	C_2H_3	–
9-epiquinidine (**9a**)	15	*R*	*R*	OCH_3	C_2H_3	–
9-epiquinine (**10a**)	21	*S*	*S*	OCH_3	C_2H_3	–
cinchonine (**9b**)	3.5	*R*	*S*	H	C_2H_3	–
cinchonidine (**10b**)	7.5	*S*	*R*	H	C_2H_3	–
6′-chlorcinchonine (**9c**)	0.52	*R*	*S*	Cl	C_2H_3	–
6′-chlorcinchonidine (**10c**)	3.5	*S*	*R*	Cl	C_2H_3	–
10,11-dihydroquinidine (**9d**)	0.066	*R*	*S*	OCH_3	C_2H_5	–
10,11-dihydroquinine (**10d**)	4.0	*S*	*R*	OCH_3	C_2H_5	–
N-benzylquinium chloride (**10e**)	25	*S*	*R*	OCH_3	C_2H_3	benzyl
quininone (**10f**)	0.72	*S*	–	OCH_3	C_2H_3	–

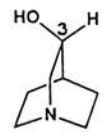

Quinuclidinol

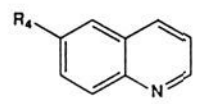

Quinoline and derivatives

inhibitor	K_i (μM)	R_4
3-quinuclidinol (**11**)	>1000	–
quinoline (**12a**)	>1000	H
6-methoxyquinoline (**12b**)	>1000	OCH_3

[a] K_i: apparent inhibition constant.

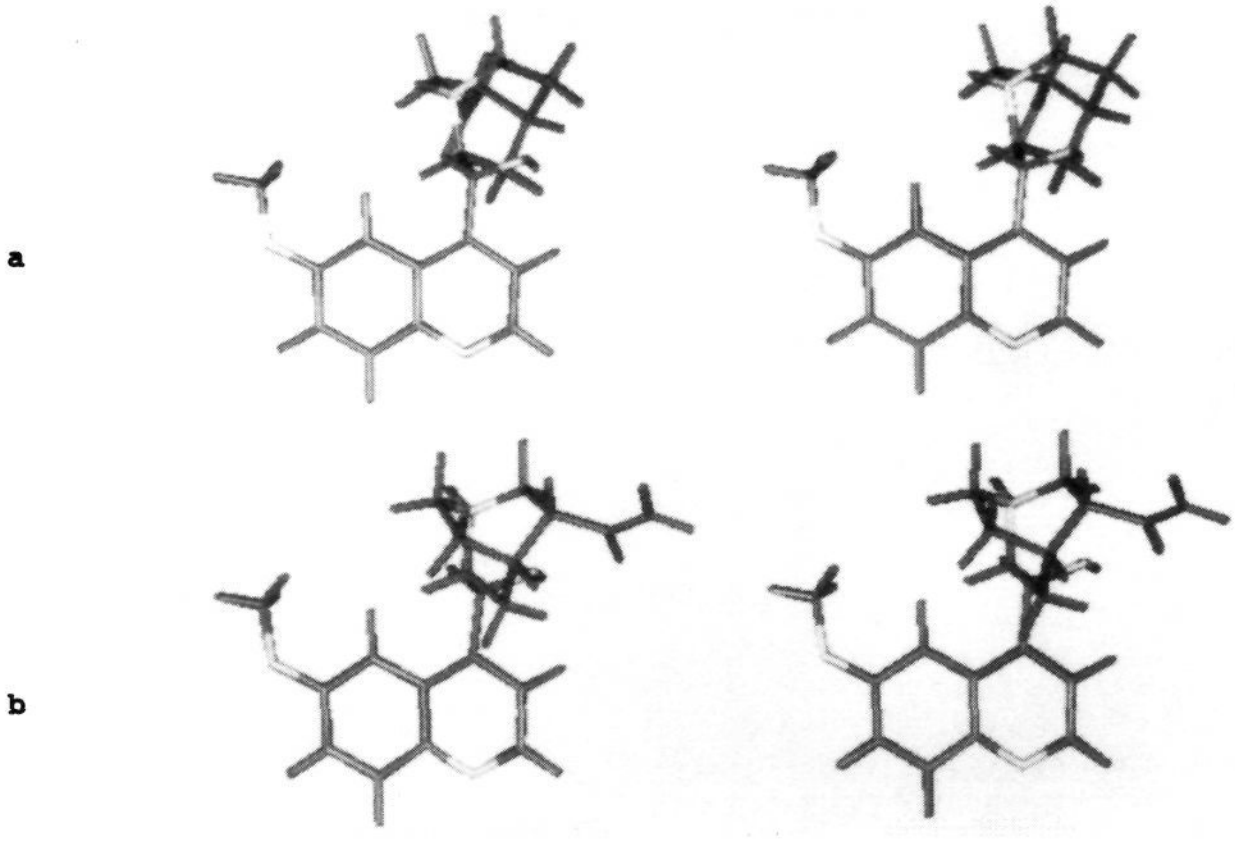

Figure 5. Stereoview of the X-ray structures of (a) quinine (**10**) and (b) quinidine (**9**).

former of **10** and the inhibitory potency was only slightly lower than that of **10**. On the other hand, **9a** was 2 orders of magnitude less potent than **9**. Conformational analysis yielded a conformer of **9a** that can be fit within the pharmacophore model, but no conformer was found that resembles **9**. In the latter case, an overlap would occur of hydrogen atoms of the quinoline and quinuclidine ring system with the oxygen and hydrogen atom of the hydroxyl group. The interchange of the vinyl group for an ethyl group neither had a great influence on the structure nor on the potency of inhibition of the compounds. The fact however, that there is a positive potential in the area of the ethyl groups of 10,11-dihydroquinidine (**9d**) and 10,-11-dihydroquinine (**10d**) suggests that it is not the presence of a negative molecular electrostatic potential that is a prerequisite for an inhibition of cytochrome P-450 2D6, but the presence of a flat hydrophobic group.

Conformational analyses and molecular dynamics calculations indicate that the structure of *N*-benzylquininium chloride (**10e**) is rather rigid. The lowest-energy conformer

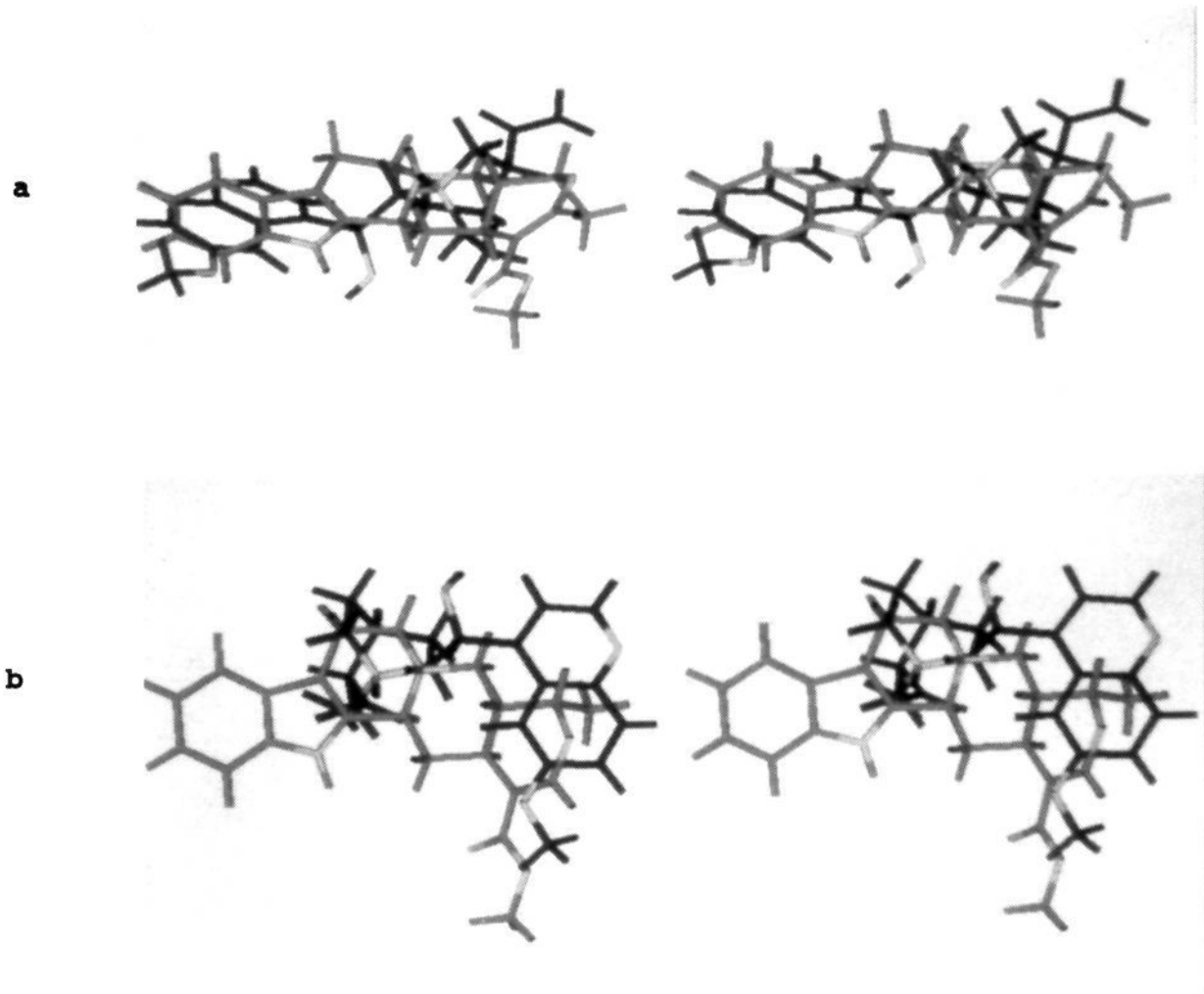

Figure 6. Stereoview of the superposition of quinine (**10**) conformers and ajmalicine (**1**). (a) Superposition of a conformer with an energy 4 kcal/mol above the global energy minimum on **1** according to the pharmacophore requirements. Note that the hydrogen bond accepting groups of **10** and **1** lie in different regions. (b) Conformer with the lowest energy superimposed on **1**. Note that the hydrogen bond accepting groups of **10** and **1** lie in the same regions but the pharmacophore requirements are not met.

could be fit within the pharmacophore model with the phenyl ring situated in region A and the vinyl group in the second hydrophobic region (C). Nevertheless, the K_i of **10e** was higher than that of **10**, probably because the positive charge of the ammonium ion is not directed.

The high potency of inhibition of quininone (**10f**) was unexpected because its low-energy conformers resemble those of **10**. The explanation for the strong inhibition is provided by the fact that **10f** shows mutarotation in solution.[36,37] At equilibrium, 22% exist as the epimeric quinidinone,[38] which could be fit within the pharmacophore model quite as well as **9**.

Conclusions

Molecular modeling studies in conjunction with inhibition studies strongly indicate that the pharmacophore is defined by a positive charge on a nitrogen atom and a flat hydrophobic region (A) that maximally extends up to a distance of 7.5 Å from this nitrogen atom (Figure 8). Compounds showing only these minimum requirements were only weak inhibitors, however. A higher inhibitory potency was observed when additional groups with a negative molecular electrostatic potential and hydrogen bond acceptor properties were present in region B at distances of 4.8–5.5 Å and 6.6–7.5 Å from the nitrogen atom, respectively. Some inhibitors also occupied space in region C. The K_i values of these compounds suggest that interaction in this region is allowed, but does not lead to a higher affinity. A superposition of low-energy conformers of all inhibitors discussed in this paper is presented in Figure 9. This model also includes weak inhibitors. The grid shows the combined molecular surface of all inhibitors and represents the excluded volume, i.e. the space available at the active site for the binding of inhibitors. Compounds that took additional space were not inhibitors. An example in this respect is reserpine (**17**),[17] which resembles **1** in the area of rings A to E but has an additional ring that extended beyond the excluded volume map (Figure 10).

To our knowledge, this is the first pharmacophore model for inhibitors of a cytochrome P-450 enzyme. On the basis of this 3-dimensional model, it is possible to explain the different potencies of compounds to inhibit cytochrome P-450 2D6-dependent reactions. The possibility to predict potencies of inhibition is being examined, and so far the results suggest that one can classify compounds semiquantitatively according to their potency to inhibit cytochrome P-450 2D6-dependent reactions. This approach may contribute to the understanding of drug interactions and to an improvement of drug safety.

Experimental Section

Biochemistry. Purification of Cytochrome P-450 2D6. Human liver microsomes were prepared from livers of healthy donors according to the method described by Guengerich.[20] The purification was done according to the method of Distlerath et al.[21] with some modifications. Briefly, microsomes were solubilized with sodium cholate and applied to *n*-octylamino Sepharose 4B columns (2.5 × 40 cm). The columns were then washed with 0.1 M potassium phosphate buffer (pH 7.25) containing 1 mM EDTA, 0.42% sodium cholate (w/v), and 20% glycerol (v/v). Most of the cytochrome P-450 enzymes were eluted with 0.1 M potassium phosphate buffer (pH 7.25) containing 1 mM EDTA, 0.33% sodium cholate (w/v), 20% glycerol (v/v), and 0.06% Emulgen 911 (w/v). Subsequently, the fraction containing cytochrome P-450 2D6 was eluted with 0.1 M potassium phosphate buffer (pH 7.25) containing 1 mM EDTA, 0.33% sodium cholate (w/v), 20% glycerol (v/v), and 0.5% Emulgen 911 (w/v). The purification was monitored after each step by immunoblots[39] and by determination of bufuralol 1′-hydroxylase activity[23] in the reconstituted enzyme system. The amount of cytochrome P-450 and cytochrome P-420 was determined according to Omura & Sato.[40] The fractions containing cytochrome P-450 2D6 were dialyzed versus 20% glycerol (v/v), applied to a hydroxyapatite column (2.5 × 10 cm), and eluted

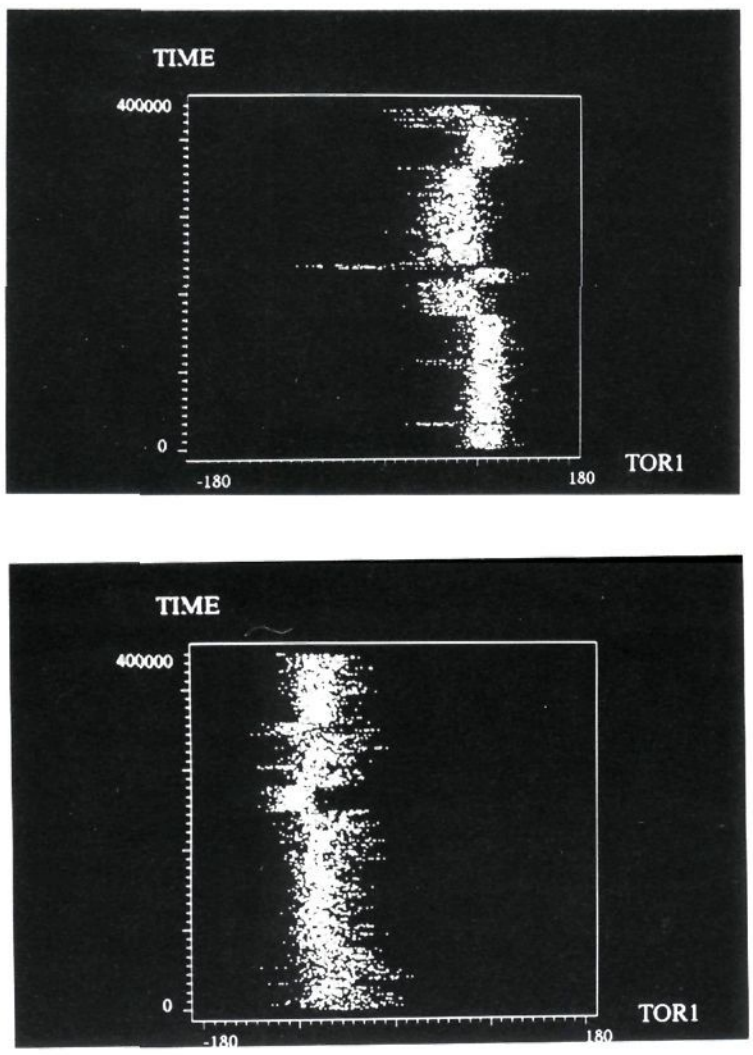

Figure 7. Molecular dynamics calculations for (a) quinine (**10**) and (b) quinidine (**9**) at 300 K for 400 ps. Temporal distribution of the value of the torsion angle 8–9–4′–3′. Note that for **9** there are only minor changes of the torsion angle. For **10** a major change occurs once but it is not due to a complete rotation of the quinuclidine ring to the opposite side. The resulting conformation of **10** is very different from that of **9**.

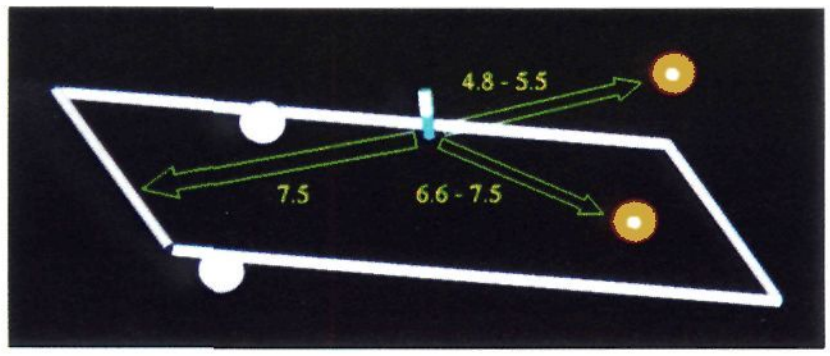

Figure 8. View of the pharmacophore and the groups supposed to enhance the potency of inhibition. The plane of the hydrophobic region is represented by the rectangle. The points on the normal to the ring plane are shown on the left side. The protonated nitrogen atom is shown in the middle (N: blue; H: cyan). The orange points on the right side symbolize the heteroatoms supposed to enhance the potency of inhibition. The distance ranges are given in angstroms.

with a stepwise gradient of increasing phosphate concentration. The buffer contained 0.3% Emulgen 911 (w/v), 20% glycerol (v/v), and 10, 20, 40, 60, or 90 mM phosphate buffer (pH 7.4), increasing in order. The fractions with high bufuralol 1′-hydroxylase activity (10 and 20 mM phosphate eluates) were dialyzed versus 20% glycerol (v/v) and stirred with Amberlite XAD-2 beads to remove detergent. The fractions were concentrated 5-fold using an Amicon PM-30 ultrafiltration cell (Amicon, Lexington, MA) and stored at −20 °C.

Inhibition Studies. The incubations were carried out using 40 μL of human liver microsomes containing 50 pmol of cytochrome P-450, 20 μL of 1 M phosphate buffer pH (7.4), 25 μL of (±)-bufuralol hydrochloride (**18**; 3 concentrations: 20–80 nmol), and 40 μL of an inhibitor solution. The inhibitor was included at 3 or 5 different concentrations which were determined by means of a preliminary screening. Distilled water was added to a final volume of 200 μL. After preincubation at 37 °C for 3 min, the reaction was started by addition of 40 μL of an NADPH-

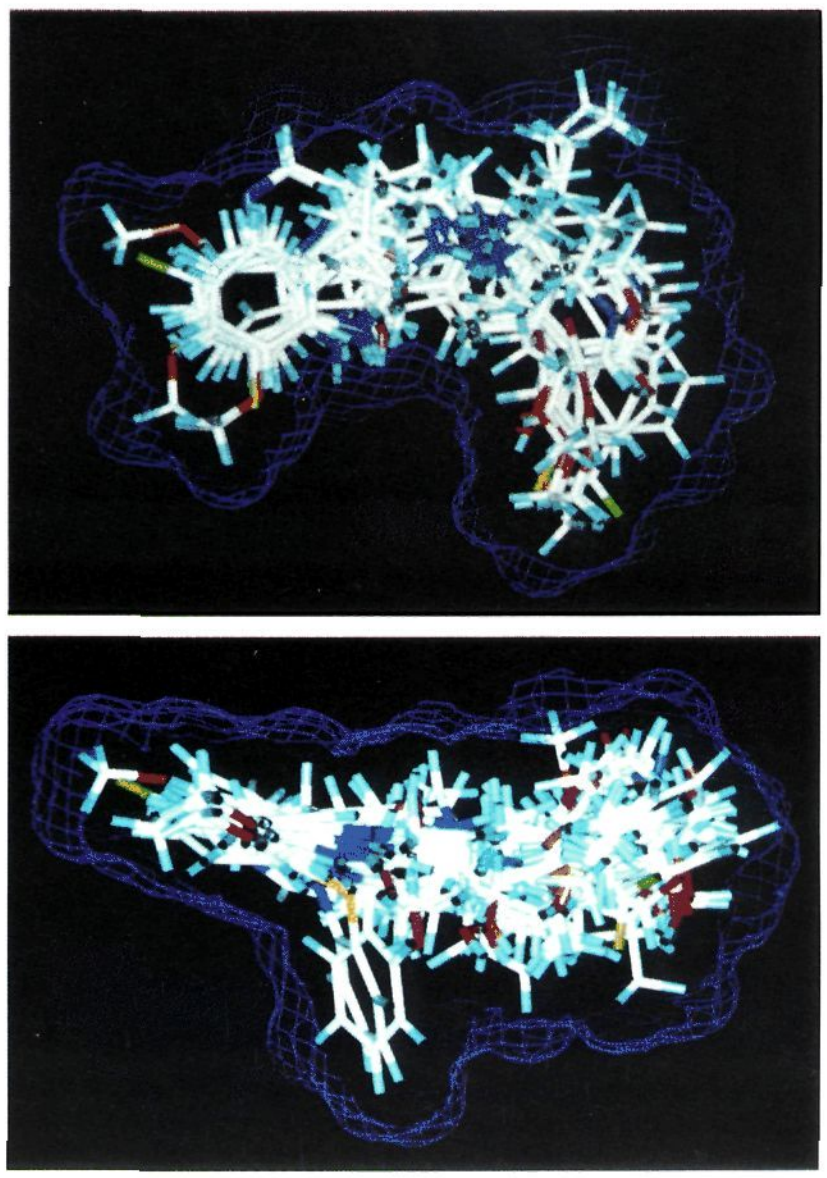

Figure 9. Superposition of low-energy conformers of all inhibitors tested in this study. (a, top) Top view of the molecule plane; (b, bottom) after 90° turn around the *x* axis. The Z-clipped grid represents the overall surface of the structures shown. Colors: C: white; H: cyan; N: dark blue; O: red; S: yellow; F, Cl: green.

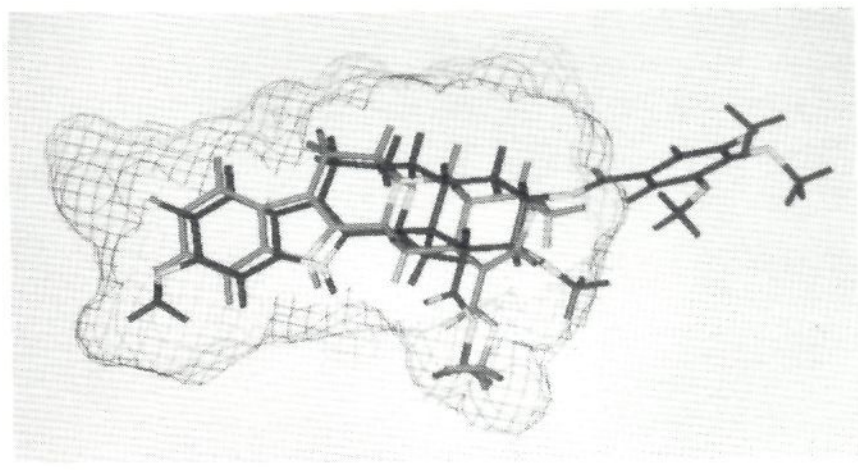

Figure 10. Superposition of reserpine (**17**) and ajmalicine (**1**). The Z-clipped grid represents the overall surface of all inhibitors.

generating system containing 0.4 mM $NADP^+$, 6 mM glucose 6-phosphate, and 5.6 units glucose 6-phosphate dehydrogenase/mL. After 30 min the reaction was stopped by addition of 20 μL of 60% $HClO_4$ (w/v). The samples were centrifuged for 10 min at 12 000 rpm (Sigma 201M, Osterode, Germany) and the supernatants were analyzed immediately or stored at −16 °C. All points were determined in duplicate.

When incubations were carried out using purified cytochrome P-450 2D6, the concentrations of buffer, substrate, inhibitor, cofactors, and cytochrome P-450 were as above, and 6 nmol of sonicated L-α-dilauroyl-*sn*-glycero-3-phosphocholine and 200–500 pmol of rabbit liver NADPH-cytochrome P-450-reductase were added to the reaction mixture.

1′-Hydroxybufuralol (**19**), the main metabolite of the reaction of cytochrome P-450 2D6 with bufuralol (**18**), was separated by high performance liquid chromatography using a Beckman gradient system (114 M pumps, Beckman, Munich, Germany). The reversed-phase ion pair chromatographic method of Kronbach et al.[23] was modified. Aliquots (15 μL) of the protein-free

samples were injected by means of an autosampler (231-401, Gilson, Villiers le Bel, France). The *n*-octadecylsilane column (Spherisorb ODS II, 5 μm, 250 × 4.6 mm, Bischoff, Leonberg, Germany) was eluted isocratically with eluent I which consisted of 35% acetonitrile and 65% water containing 0.2 M $NaClO_4$ and which was adjusted to pH 4 using $HClO_4$. To elute more lipophilic compounds (including 18), a gradient was initiated after 3 min, increasing to 60% eluent II (90% CH_3OH and 10% tetrahydrofuran, v/v). After 5.5 min, a gradient was initiated, increasing to 100% eluent I. 19 was detected by means of a fluorescence monitor (RF-535, Shimadzu, Egling, Germany) using an excitation wavelength of 252 nm and an emission wavelength of 302 nm. The peaks were recorded and quantified with an integrator (4290, Varian, Munich, Germany). The area was proportional to the injected amount of 19 in the range of 1.75 and 65 pmol of the metabolite. The type of inhibition and the inhibition constant K_i was determined by means of Dixon plots.[22] In case of equivocal results the type of inhibition was checked by evaluation of the data according to Cornish-Bowden.[41]

Chemistry

Compounds 1, 6b, 6c, 7a, 7b, 8, 10, and 11 were purchased from Serva Feinbiochemica GmbH & Co, Heidelberg, Germany, compounds 1c and 1d were gifts of Prof. Husson, CNRS, Gif sur Yvette, France, 2 was obtained from the isotope laboratory of the Institute of Pharmaceutical Biology, University of Munich, Germany, 4 and 12b were purchased from Aldrich-Chemie GmbH & Co. KG, Steinheim, Germany, 4b and 9 were purchased from Carl Roth GmbH & Co, Karlsruhe, Germany, 4c was a gift of Dr. Burgdorf, Buchler-Chemie, Braunschweig, Germany, 5 was purchased from ICN Biomedicals GmbH, Meckenheim, Germany, 6a was purchased from Sigma Chemie GmbH, Deisenhofen, Germany, 9a, 10a, 9c, 10c, 9d, 10d, 18, 19, 18a, and 18b were gifts of Hofmann-La Roche, Basel, Switzerland, 9b, 10b, 10f, 9e, and 10g were gifts of Boehringer Mannheim GmbH, Mannheim, Germany, 10e was purchased from E. Merck AG, Darmstadt, Germany, and 12a was purchased from Fluka Feinchemikalien GmbH, Neu-Ulm, Germany.

Synthesis of Indole Alkaloids. 16,17-Didehydro-16-(hydroxymethyl)-19-methyloxayohimban (1a): 50 mg (142 μmol) ajmalicine (1) was refluxed in dry ethyl ether under He in the presence of 15 mg $LiAlH_4$ for 2 h. After hydrolysis of this mixture with H_2O, the organic layer was purified on TLC (0.5 mm; Si 60-F_{254}, Merck, Darmstadt) with the solvent system petroleum ether/acetone/diethylamine (7:2:1); 20 mg (59 μmol) of 1a was obtained (yield 42%) showing a purity by TLC > 97% (R_f = 0.40 in the same solvent system) and showing the following MS data (major fragments are given): EI-MS, *m/z* (rel inten %) 325 (M^+ + 1, 24); 324 (M^+, 100); 323 (63); 322 (17); 306 (13); 305 (11); 209 (23); 185 (20); 184 (64); 183 (23); 169 (26); 156 (41); 144 (9); 143 (9); HR-MS: M^+ 324.1830, $C_{20}H_{24}N_2O_2$ requires 324.1837.

Tetrahydroalstonine (1b) was prepared by reduction of alstonine (34.8 mg, 100 μmol) in 1 mL methanol and excess of $NaBH_4$. Chromatography of this mixture on 0.5 mm silica gel plates with the solvent system ethyl acetate/ether/*n*-hexane (2:2:1; R_f = 0.92) furnished 26.4 mg of 1b (75% yield): mp 227–229 °C (MeOH); MS data (major fragments are given) EI-MS, *m/z* (rel inten %) 352 (M^+, 100); 351 (84); 223 (18); 222 (19); 184 (34); 169 (28); 156 (70).

16-(Hydroxymethyl)-17-hydroxyyohimban (4a): starting with yohimbine and applying the same conditions as for the synthesis of 1a the yohimbine alcohol 4a was obtained in 40% yield (TLC purity: 98%; solvent system petroleum ether/acetone/diethylamine, R_f = 0.21); EI-MS *m/z* (rel inten %) 327 (M^+ + 1, 13); 326 (M^+, 100); 325 (82); 324 (21); 184 (13); 169 (27); 156 (15); 144 (17); 143 (13); HR-MS M^+ 326.1989, $C_{20}H_{26}N_2O_2$ requires 326.1994.

Cathenamine (3) was enzymatically prepared from the glucoalkaloid strictosidine and purified according to a published method.[43]

Mass spectra were measured on a Finnigan MAT 44S quadrupole instrument at 70 eV.

Acknowledgment. The financial support of the Deutsche Forschungsgemeinschaft (SFB 145) and of the Fonds der Chemischen Industrie is gratefully acknowledged. We wish to thank Dr. Kaiser and Dr. Gutmann, Hofmann-La Roche, Dr. Kuhr, Boehringer Mannheim, Dr. Burgdorf, Buchler AG, Prof, Dr. Husson, CNRS, and Dr. Sarlet, Omnichem for kindly providing numerous compounds and Dr. H. Münster, Finnigan MAT for high resolution mass spectra.

Supplementary Material Available: Selected torsion angles of low-energy conformers of 13 (Table I), 14 (Table II), 16 (Table III), 9 (Table IV), 10 (Table V), 9a (Table VI), 10a (Table VII), 10e (Table VIII), and 10f (Table IX) (9 pages). Ordering information is given on any current masthead page.

References

(1) Lu, A. Y. H.; West, S. B. Multiplicity of Mammalian Microsomal Cytochromes P-450. *Pharmacol. Rev.* **1980**, *31*, 277–295.
(2) Eichelbaum, M. Defective Oxidation of Drugs: Pharmacokinetic and Therapeutic Implications. *Clin. Pharmacokinet.* **1982**, *7*, 1–22.
(3) Clark, D. W. J. Genetically Determined Variability in Acetylation and Oxidation. Therapeutic Implications. *Drugs* **1985**, *29*, 342–375.
(4) Price-Evans, D. A.; Mahgoub, A.; Sloan, T. P.; Idle, J. R.; Smith, R. L. A Family and Population Study of the Genetic Polymorphism of Debrisoquine Oxidation in a British Population. *J. Med. Genet.* **1980**, *17*, 102–105.
(5) Peart, G. F.; Boutagy, J.; Shenfield, G. M. Debrisoquine Oxidation in an Australian Population. *Br. J. Clin. Pharmacol.* **1986**, *21*, 465–471.
(6) Benitez, J.; Lerena, A.; Cobaleda, J. Debrisoquin Oxidation Polymorphism in a Spanish Population. *J. Clin. Pharmacol. Ther.* **1988**, *44*, 74–77.
(7) Shah, R. R.; Oates, N. S.; Idle, J. R.; Smith, R. L.; Lockhart, D. F. Impaired Oxidation of Debrisoquine in Patients with Perhexiline Neuropathy. *Br. Med. J.* **1982**, *284*, 295–299.
(8) Siddoway, L. A.; Thompson, U. A.; McAllister, B.; Wang, T.; Wilkinson, G. R.; Roden, D. M.; Woosley, R. L. Polymorphism of Propafenone Metabolism and Disposition in Man: Clinical and Pharmacokinetic Consequences. *Circulation* **1987**, *75*, 785–791.
(9) Eichelbaum, M.; Gross, A. S. The Genetic Polymorphism of Debrisoquine/Sparteine Metabolism. Clinical Aspects. *Pharmacol. Ther.* **1990**, *46*, 377–394.
(10) Otton, S. V.; Inaba, T.; Kalow, W. Competitive Inhibition of Sparteine Oxidation in Human Liver by β-Adrenoceptor Antagonists and Other Cardiovascular Drugs. *Life Sci.* **1984**, *34*, 73–80.
(11) Brosen, K.; Gram, L. F.; Haghfelt, T.; Bertilsson, L. Extensive Metabolizers of Debrisoquine Become Poor Metabolizers during Quinidine Treatment. *Pharmacol. Toxicol.* **1987**, *60*, 312–314.
(12) Steiner, E.; Dumont, E.; Spina, E.; Dahlqvist, R. Inhibition of Desipramine 2-Hydroxylation by Quinidine and Quinine. *Clin. Pharmacol. Ther.* **1988**, *43*, 577–581.
(13) Leemann, T.; Dayer, P.; Meyer, U. A. Single-Dose Quinidine Treatment Inhibits Metoprolol Oxidation in Extensive Metabolizers. *Eur. J. Clin. Pharmacol.* **1986**, *29*, 739–741.
(14) Brinn, R.; Brosen, K.; Gram, L. F.; Haghfelt, T.; Otton, V. Sparteine Oxidation is Practically Abolished in Quinidine-treated Patients. *Br. J. Clin. Pharmacol.* **1986**, *22*, 194–197.
(15) Otton, S. V.; Inaba, T.; Kalow, W. Inhibition of Sparteine Oxidation in Human Liver by Tricyclic Antidepressents and Other Drugs. *Life Sci.* **1983**, *32*, 795–800.
(16) Inaba, T.; Jurima, M.; Mahon, W. A.; Kalow, W. In vitro Inhibition Studies of Two Isozymes of Human Liver Cytochrome P-450 – Mephenytoin p-Hydroxylase and Sparteine Monooxygenase. *Drug Metab. Disp.* **1985**, *13*, 443–448.
(17) Fonne-Pfister, R.; Meyer, U. A. Xenobiotic and Endobiotic Inhibitors of Cytochrome P-450db1 Function, the Target of the Debrisoquine/Sparteine Type Polymorphism. *Biochem. Pharmacol.* **1988**, *37*, 3829–3835.
(18) Olsen, E. C.; Christoffersen, R. E., Eds. *Computer-Assisted Drug Design*; ACS Symposium Series 112, American Chemical Society, Washington, D.C., 1979.
(19) Marshall, G. R. Computer-Aided Drug Design. *Ann. Rev. Pharmacol. Toxicol.* **1987**, *27*, 193–213.

(20) Guengerich, F. P. Microsomal Enzymes Involved in Toxicology – Analysis and Separation. In *Principles and Methods of Toxicology*; Hayes, W. A., Ed.; Raven Press: New York, 1982; pp 609–634.
(21) Distlerath, L. M.; Reilly, P. E. B.; Martin, M. V.; Davis, G. G.; Wilkinson, G. R.; Guengerich, F. P. Purification and Characterization of the Human Liver Cytochromes P-450 Involved in Debrisoquine 4-Hydroxylation and Phenacetin O-Deethylation, Two Prototypes for Genetic Polymorphism in Oxidative Drug Metabolism. *J. Biol. Chem.* **1985**, *260*, 9057–9067.
(22) Dixon, M. The Determination of Enzyme Inhibitor Constants. *Biochem. J.* **1953**, *55*, 170–171.
(23) Kronbach, T.; Mathys, D.; Gut, J.; Catin, T.; Meyer, U. A. High-Performance Liquid Chromatographic Assays for Bufuralol 1'-Hydroxylase, Debrisoquine 4-Hydroxylase, and Dextromethorphan O-Demethylase in Microsomes and Purified Cytochrome P-450 Isozymes of Human Liver. *Anal. Biochem.* **1987**, *162*, 24–32.
(24) Allen, F. H.; Bellard, S.; Brice, M. D.; Cartwright, B. A.; Doubleday, A.; Higgs, H.; Hummelink, T.; Hummelink-Peters, B. G.; Kennard, O.; Motherwell, W. D. S.; Rodgers, J. R.; Watson, D. G. The Cambridge Crystallographic Data Centre: Computer-Based Search, Retrieval, Analysis and Display of Information. *Acta Crystallog. Sect. B: Struct. Crystallogr. Cryst. Chem.* **1979**, *35*, 2331–2341.
(25) Tripos Associates, Inc., St. Louis, MO 63144.
(26) Dewar, M. J. S.; Thiel, W. Ground States of Molecules. 38. The MNDO Method. Approximations and Parameters. *J. Am. Chem. Soc.* **1977**, *99*, 4899–4907. The version used was VAMP 4.1 vectorized by Clark, T., Erlangen.
(27) Gut, J.; Catin, T.; Dayer, P.; Kronbach, T.; Zanger, U.; Meyer, U. A. Debrisoquine/Sparteine-type Polymorphism of Drug Oxidation. *J. Biol. Chem.* **1986**, *261*, 11734–11743.
(28) Hübner, T., unpublished results.
(29) Suszko-Purzycka, A.; Lipinska, T.; Piotrowska, E. 10-Hydroxy-10-methyl-10,11-dihydroquinine, C21H28N2O3, a New Derivative of Quinine. *Acta Crystallogr. Sect. C: Cryst. Struct. Commun.* **1985**, *41*, 977–980.
(30) Doherty, R.; Benson, W. R.; Maienthal, M.; Stewart, J. Crystal and Molecular Structure of Quinidine. *J. Pharmaceut. Sci.* **1978**, *67*, 1698–1701.
(31) Kashino, S.; Haisa, M. Structure of Quinidine, C20H24N2O2. *Acta Crystallogr. Sect. C: Cryst. Struct. Commun.* **1983**, *39*, 310–312.
(32) Oleksyn, B. J.; Lebioda, L.; Ciechanowicz-Rutkowska, M. The Molecular and Crystal Structure of the Alkaloid Cinchonine. *Acta Crystallogr. Sect. B: Struct. Crystallogr. Cryst. Chem.* **1979**, *35*, 440–444.
(33) Suszko-Purzycka, A.; Lipinska, T.; Karczmarzyk, Z.; Pniewska, B. J. 10-Hydroxy-10-methyl-10,11-dihydroquinidine. *Cryst. Spectrosc. Res.* **1987**, *17*, 31–40.
(34) Schripsema, J.; Verpoorte, R.; Baerheim Svendsen, A.; Erkelens, C. Natural Abundance Nitrogen-15 NMR: A Study About the Conformation and Protonation Site of Some Quinoline Alkaloids. *Spectrosc. Lett.* **1987**, *20*, 777–784.
(35) Diaz-Arauzo, H.; Cook, J. M.; Christie, D. J. Syntheses of 10,11-Dihydroxydihydroquinidine N-Oxide, a new Metabolite of Quinidine. Preparation and H-NMR Spectroscopy of the Metabolites of Quinine and Quinidine and Conformational Analysis. *J. Nat. Prod.* **1990**, *53*, 112–124.
(36) Woodward, R. B.; Wendler, N. L.; Brutschy, F. J. Quininone. *J. Am. Chem. Soc.* **1945**, *67*, 1425–1429.
(37) Gutzwiller, J.; Uskokovic, M. R. Reinvestigation of the Classical Synthesis of Cinchona Alkaloids. II. The Synthesis of Quinine and its Naturally Occuring Diastereomers from Quinotoxine. *Helv. Chim. Acta* **1973**, *56*, 1494–1503.
(38) Robins, R. J.; Rhodes, M. J. C. An Evaluation of the Tautomerism of Cinchoninone and Quinidinone Made Using a Combination of 1H NMR and 13C NMR Spectroscopy. *Phytochemistry* **1987**, *26*, 551–556.
(39) Guengerich, F. P.; Wang, P.; Davidson, N. K. Estimation of Isozymes of Microsomal Cytochrome P-450 in Rats, Rabbits, and Humans Using Immunochemical Staining Coupled with Sodium Dodecyl Sulfate-Polyacrylamide Gel Electrophoresis. *Biochemistry* **1982**, *21*, 1698–1706.
(40) Omura, T.; Sato, R. The Carbon Monoxide-Binding Pigment of Liver Microsomes. I. Evidence for its Hemoprotein Nature. *J. Biol. Chem.* **1964**, *239*, 2370–2378.
(41) Cornish-Bowden, A. A Simple Graphical Method for Determining the Inhibition Constants of Mixed, Uncompetitive and Non-Competitive Inhibitors. *Biochem. J.* **1974**, *137*, 143–144.
(42) Griffith, W. P.; Ley, S. V.; Withcombe, G. P.; White, A. D. Preparation and Use of Tetra-n-butylammonium Per-ruthenate (TBAP reagent) and Tetra-n-propylammonium Per-ruthenate (TPAP reagent) as New Catalytic Oxidants of Alcohols. *J. Chem. Soc., Chem. Commun.* **1987**, 1625–1627.
(43) Stöckigt, J. Enzymatic Formation of Intermediates in the Biosynthesis of Ajmalicine: Strictosidine and Cathenamine. *Phytochemistry* **1979**, *18*, 965–971.